FEATURE-BASED SENSING MATRIX DESIGN FOR ANALOG TO INFORMATION CONVERTERS

Chencheng Guo, Hui Qian, Baoling Hong*

College of Physics and Information Engineering, Fuzhou University, Fuzhou, China

ABSTRACT

In this paper, we propose a novel sensing matrix design for the pulse-width modulation (PWM)-based analog-to-information converter (AIC), which obtains the digital feature of an analog signal rather than its sparse coefficients. The method firstly selects feature subsets by feature selection algorithm of support vector machines (SVMs) and then establishes the relationship between feature subsets and the vector of sensing matrix of PWM-based AIC. Then, a sensing matrix with a higher compression ratio can be obtained. The new optimized sensing matrix is mapped to the reference modulation sequence of the PWM-based AIC's modulation signal to obtain the PWM-based analog-to-feature converter (AFC). Experimental results show that the PWM-based AFC can reach 99.40% accuracy even when the compression ratio is higher than that of other literature.

Index Terms— Compressed sensing, AIC, Analog-to-Feature converter, SVMs, PWM

1. INTRODUCTION

Analog-to-information converter (AIC) is an emerging signal acquisition technology [1] [2] [3], which directly extracts the information from an analog signal at a rate below Nyquist. With its much lower data rate, AIC has been since attracted extensive attention of the internet of things (IoT) [4] [5] [6], notably the medical IoT. In these applications, the classifier, such as support vector machines (SVMs), can lower its power consumption by using the compressed AIC measurements of physical signals[7]. In recent years, Hardware-Software Co-design has been applied to this field [8] [9]. Although this approach can save a lot of power consumption [10], it is not very efficient because the goal of AIC is to reconstruct the original signal rather than classify it [11].

In the current AIC based on classification systems, AIC first maps an analog signal to the digital measurements at a sub-Nyquist rate, and the AIC's measurements are input to the classifier. Recently, researchers have found that the classifier still discards some redundant AIC measurements [12]. It indicates that the feature bandwidth may be much lower than the information bandwidth. The feature is a special kind of information. In 2015, M.Verhelst et al. first proposed the idea of analog-to-feature converter (AFC) [12]. The AFC based on the ECG acquisition system has been realized in [13] [14]. Especially, [14] confirmed that AFC can save at least 70% computing resources compared with the classical method of AIC sampling followed by feature extraction of the compressed domain.

This paper proposes a PWM-AFC structure based on the basic method of SVMs nonlinear data classification. In this system, based on the design of PWM-AIC [3] [15], the sawtooth signal is used as a modulation signal, SVM-oriented PWM width parameters are obtained through offline training, and the design of the AFC sensing matrix is realized. In order to analyze the performance of the system, a simulation platform of the PWM-AFC system under the MATLAB/SIMULINK was built in this paper. Based on the ECG signals in the MIT-BIH database [16], the system was trained and verified.

2. PROBLEM FORMULATION

2.1. The Basic Structure of AIC

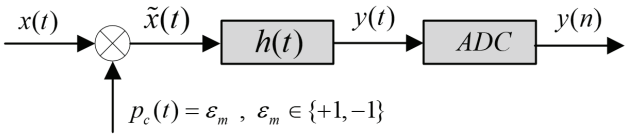

Fig. 1. the structure of RD AIC

Single-channel random demodulation (RD) AIC sampling framework for discrete multi-tone signals based on the basic principle of CS was proposed in [1] [2]. As shown in Fig. 1, the method uses random sequence $p_c(t)$ to demodulate the input signal $x(t)$ randomly, and then integrates and samples the demodulation signal $\tilde{x}(t)$ to get the final output samples. AIC integrates and samples demodulated signals at T_c seconds interval, supposing the impulse response of the low-pass filter is $h(t)$, AIC obtains $N = 1/T_c$ samples in the unit interval,

* This work was supported by the Digital Fujian Key Laboratory of IoT Engineering and Applications under Grant No. 82917002. (Corresponding author: Hui Qian)

and the output samples $y[n]$ can be expressed as

$$\begin{array}{l} y(n) = y(t)|_{t=nT_c} = \tilde{x}(t) * h(t) \\ = \int_{(n-1)T_c}^{nT_c} x(\tau) p_c(\tau) h(t-\tau) d\tau, n = 1, 2, ..., N \end{array} . \quad (1)$$

Defining that the compression ratio of AIC is $L = W/N$, Eq. (1) can be expressed as

$$y(n) = \sum_{l=1}^{L} \sum_{k=0}^{W-1} \int_{(n-1)l/W}^{((n-1)l+1)/W} c_k \varepsilon_l \exp(-j2\pi kt) d\tau \ . \quad (2)$$

Expressing the above equation in terms of Fourier coefficients and Fourier bases

$$y(n) = \sum_{l=1}^{L} \sum_{k=0}^{W-1} \alpha_k \phi_k(n) \varphi_{l,n}(n), \quad (3)$$

respectively, α_k and $\phi_k(n)$ express the discrete-time Fourier coefficients and the Fourier basis, and $\varphi_{l,n}(n)$ represents the sensing matrix of AIC. So the outputs of AIC can be expressed in the form of vectors as follows

$$Y = \Phi \Psi A, \quad (4)$$

where Y and A denote an N-dimensional vector and a sparse W-dimensional vector respectively; Ψ is a W-dimensional vector; Φ is an $N \times W$-dimensional sensing matrix. The solution process of Eq. (4) is a typical NP problem. According to CS, the vector A can be reconstructed from measurement vectors Y when the sensing matrix meets restricted isometry property (RIP) conditions. The approximate solution of the sparse coefficient can be obtained by solving the following expression

$$\hat{A} = \arg\min \|Y - \Phi \Psi A\|_2^2 + \lambda \|A\|_1 , \quad (5)$$

where $\lambda (0 < \lambda < 1)$ is the penalty parameter.

2.2. SVM and AIC

According to the above analysis, AIC can obtain the measurement samples Eq. (4), which can be obtained by designing the sensing matrix Φ. Based on the principle of SVMs, this paper discusses the architecture of extracting digital features directly from analog signals. Given a set of samples $y[n]$ and corresponding markers $\{q_n\}$, the kernel function $K(\cdot)$ is used to map the samples into the linearly separable space, namely $y[n] \to K(\cdot)$. The SVMs model can be described as

$$\begin{array}{l} \lim \frac{1}{2} \|\alpha\| + C \sum_{n=1}^{P} \varepsilon_n \\ s.t. q_n(\alpha^T K(y[n]) + b) \geq 1 - \varepsilon_n \\ \varepsilon_n \geq 0, \mathrm{n} = 1, 2, ..., P \end{array} , \quad (6)$$

where $\alpha = [\alpha_1, \alpha_2, ..., \alpha_P]$ and b are the normal vectors of the hyperplane and bias, respectively. $C > 0$ is a penalty constant; $\varepsilon_i > 0$ are relaxation variables. By optimizing Eq. (6), the SVMs decision function can be obtained as

$$f(x) = sign(\sum_{n=1}^{P} \beta_n q_n K(y[n]) + b), \quad (7)$$

where β_n is the Lagrange operator. [14] First proposes the idea of SVMs combined with AIC, and ECG signals provided by the MIT-BIH are used in MATLAB to detect whether the signal is a normal heartbeat through SVMs. At the training stage of the classifier, SVMs are trained and tested for different feature dimensions. The experimental results in Table 1 shows that only 4-dimensional features can achieve an accuracy of 97.4% (related parameter explanations are in section 4.1). Obviously, it is indicated that the features of vectors in higher dimensions still have redundancy. Moreover, the redundant feature is easy to introduce noise interference, which leads to the reduction of feature separability.

Table 1. SVMs results in different feature dimensions

Dimension	P(%)	R(%)	Acc(%)
2	80.51	90.9	84.45
4	97.88	96.9	97.4
6	99.7	99.7	99.7
8	99.9	99.5	99.7
10	99.8	99.8	99.8
12	99.9	99.6	97.75

3. SYSTEM ARCHITECTURE

In this section, we propose a design of AIC sensing matrix for feature extraction, which projects the original analog signals into the sub-Nyquist feature space to further compress the feature set of the signals. To avoid the instability of RD as much as possible, this paper refers to the optimization design of the pre-quantized AIC structure based on PWM in [15] [17].

3.1. The Design of Sensing Matrix

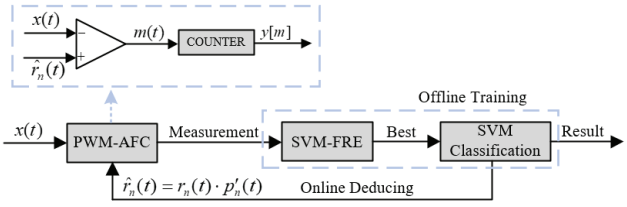

Fig. 2. the structure of PWM-AFC

As shown in Fig. 2, this paper proposes a feature conversion system based on support vector machine recursive feature elimination (SVM-RFE) [18] algorithm. In this section, we give the theoretical derivation of the sampling structure.

Algorithm 1: SVM-RFE

Input: original feature set $\{y[m]\}_{m=1}^{n}$, corresponding mark as $\{L_m\}_{m=1}^{n}$.

Output: feature set R

1 Initialization: the index $S = \{1, 2, ..., N\}$, and $R = \emptyset$;

2 Repeat the following steps until $S = \emptyset$:

3 Train the SVMs model according to the training set $\{y[m]\}_{m=1}^{n}$; Get the weight $\alpha = \alpha_1, \alpha_2, ..., \alpha_P$, and calculate the cross validation rate;

4 Calculate $J = {\alpha_i}^2$ and find out the minimum score;

5 Remove the feature vector with the lowest score and update R;

6 Find out the optimal inflection point with the following conditions

$$\begin{array}{l} s.t. \nabla X[m] \geq p, \\ \nabla X[m] \cdot \nabla X[m+1] < 0 \\ \nabla X[m+1] < 0 \end{array} . \tag{8}$$

Where p is the minimum accuracy requirement of the SVMs model, and $\nabla X[m]$ represents the first derivative of the discrete sequence X at the point m.

The sampling structure is mainly composed of a PWM-based sampler and a counter. Initially, the sawtooth wave $r_n(t)$ is used as the reference signal of the PWM, and the input signal $x(t)$ is mapped to the width τ_n of the PWM waveform $m(t)$. Finally, the selected feature information is converted into a digital sequence $y[m]$ by a counter. Since the amplitude at intersection of the input signal and the reference signal is proportional to the amplitude of the sawtooth wave, the mapping width τ_n can be expressed as

$$F(\cdot) = \tau_n = \frac{T_M}{A} x_n = \frac{T_M}{A} \int_{(n-1)T_M}^{nT_M} x(t)\delta(t - s_n)dt, \tag{9}$$

where T_M and A express the period of $r_n(t)$ and the amplitude of $x(t)$ respectively, and $s_n \in [(n-1)T_M, nT_M]$. The PN sequence $p_c(t)$ controls the counter to add or subtract, whose value is 1 or -1. The reset signal controls the compression ratio $L = W/N$, while the PWM waveform of high and low levels denotes the status of counter that 1 is counting and 0 is keeping. Therefore, the measurement value $y[m]$ of PWM with the width of τ_n can be obtained as

$$y[m] = \sum_{n=(m-1)L+1}^{mL-1} \int_{(n-1)T_M}^{nT_M} S_n^{'} x(t)dt, \tag{10}$$

where $S_n^{'} = (T_M f_b/A) p_c(t)\delta(t - s_n)$. According to Eq. (10), the dimension of $y[m]$ is equal to the compression ratio $L = W/N$. Even if the sampling system is based on Sub-Nyquist Sampling, the measurement $y[m]$ still contains a large number of redundant features. Therefore, the feature elimination algorithm based on SVM is used for optimal selection of the $y[m]$. SVM-RFE is one of the more widely used feature selection algorithms, and the specific algorithm steps are shown in Algorithm 1.

3.2. SVM Based on AFC

At the CS measurement stage, the PWM-AFC mentioned in Section 3.1 is used to extract the initial features of ECG signals. The training process is described in the following.

At the training stage, the modulation signal of the PWM is set to the product of $r_n(t)$ and $p_n'(t)$, and the optimized compression ratio is set to 7. The original 252-dimensional testing samples from the MIT-BIH are compressed into 36-dimensional measurement vectors. Then 36-dimensional measurement vectors are trained by SVM-RFE to select the feature optimal set, and a new optimal modulation signal $\hat{r}_n'(t)$ can be obtained according to the sequence mapping of the feature optimal set. At the training of SVMs stage, the penalty factor C and Gaussian kernel parameters g can be searched in the form of 2^x exponent by using 5 fold cross-validation method. At the search stage, the range of x is set to -10 to 10, the step size of the first step is 1, and the step size of the second step is 0.1. In order to avoid the over-fitting of the classifier, a smaller combination (C, g) is selected in this paper when the accuracy is approximate. So $(1, 0.8706)$ serves as the main parameter of the system. Then, the index S of the optimal feature subset is mapped into the PN sequence $p_n'(t)$ following the principle that selected is 1, otherwise 0.

According to the principle of CS, the sensing matrix Φ after feature selection can be expressed as

$$S_n^{'} = \begin{pmatrix} \Gamma\varepsilon_1, ..., \Gamma\varepsilon_L & & \\ & ... & \\ & & \Gamma\varepsilon_{(M-1)L}, ..., \Gamma\varepsilon_{ML} \end{pmatrix}, \tag{11}$$

where $[\varepsilon_1 ... \varepsilon_L]$ is the corresponding value of S mapped to the $p_n(t)$, and $\Gamma = \frac{T_M}{A} f_c$. Therefore, the reference signal can be designed as

$$\hat{r}_n(t) = r_n(t) \cdot p_n'(t), p_n'(t) = \varepsilon_m, \varepsilon_m \in \{1, 0\} \tag{12}$$

This is our optimized modulated signal.

4. EXPERIMENT RESULTS

To verify the performance of PWM-AFC, the PWM-AFC system on the Matlab R2019b/Simulink platform for simulation and the analog-digital-hybrid system on NI CompactRIO have been built in this paper.

4.1. System Simulation Analysis (SIMULINK)

Based on the MIT-BIH database, the performance of PWM-AFC is verified in this paper. In the experiment, 10000 sam-

ples are randomly selected, among which the first 5000 samples are normal heartbeat and the last 5000 samples are abnormal heartbeat. Samples of normal and abnormal heartbeats are then tagged $\{L_i\}_{i=1}^{10000}$. The dataset is divided into the training set and the testing set. 80% of the samples in the normal and abnormal heartbeat data sets are randomly selected as the training set, and the rest are the test set.

The parameters of PWM-AFC are mainly debugated on the basis of Precision (P), Recall (R) and overall classification Accuracy (Acc). Specific indicators are as follows

$$\begin{cases} P = \frac{TP}{TP+FP} \times 100\% \\ R = \frac{TP}{TP+FN} \times 100\% \\ Acc = \frac{TP+TN}{TP+TN+FP+FN} \times 100\% \end{cases} . \quad (13)$$

Normal heartbeat was taken as the target signal, and the results were shown in Table 2. In the predicted normal heartbeat, there are 4 errors, and the target signal accuracy is about 99.6%. At the prediction of non-target signal stage, there are 8 errors, the accuracy rate is 99.4%. The waveform of simulation is shown in Fig. 3 (a).

Table 2. SVM Classifier Results in SIMULINK

	Actual label		P(%)	R(%)	Acc(%)
	Positive	Negtive			
Positive	992	4	99.6	99.2	99.4
Negtive	8	996			

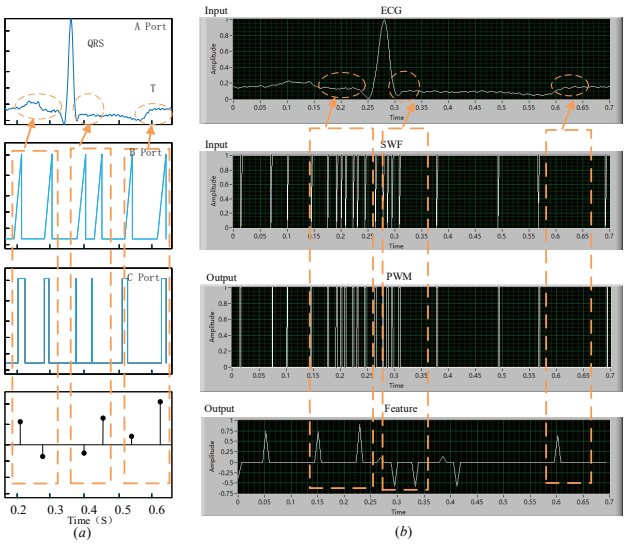

Fig. 3. (a) is the waveform of PWM-AFC in SIMULINK and (b) is the waveform in the NI CompactRIO

4.2. The Analog-and-digital Hybrid Verification

The hardware platform of the system on NI CompactRIO completes the generation of $\hat{r}_n(t)$ and the acquisition of $y[m]$ designed in this paper. Finally, the collected data is sent to the PC for direct data classification. The platform is shown in Fig. 4, which mainly includes the following processes:

(1) Generate the sawtooth signal $\hat{r}_n(t)$.
(2) Generate the PWM waveform.
(3) Data collection.
(4) Measure the value of PWM width.
(5) Feature classification in PC.

Fig. 3 (b) shows the oscillogram of signals obtained from the NI-Compact. In this paper, we also compare the literatures about ECG signals feature extraction directly in CS which is shown in Table 3. As far as the authors know, the AFC method proposed in [14] has the highest compression ratio and the best accuracy for ECG signal classification and recognition. Compared with [14], the proposed method can still achieve higher accuracy at a compression ratio of 25. Obviously, the measurement matrix designed according to the SVMs classification and recognition task, can not only improve the compression ratio of features but also ensure the classification accuracy.

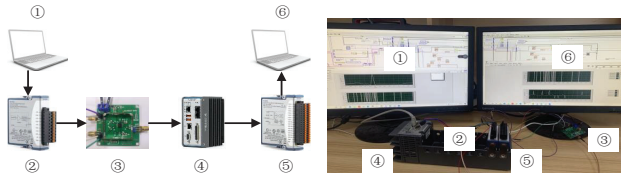

Fig. 4. ① and ⑥ are the displays; ② is the NI-9263 module used to generate sawtooth signal; ③ is the PWM modulation; ④ is the NI CompactRIO chassis used to count; ⑤ is the NI-9025 module used to receive the count value.

Table 3. SVMs results in different feature dimensions

Method	Classifier	Compression	Acc(%)
Walsh-Hadamard [14]	SVMs	16	97.5
Heart Rate Variability (HRV)[19]	SVM	10	96
PWM-AIC(This paper)	SVM	25	99.40

5. CONCLUSION

This paper proposes a novel sensing matrix design for the PWM-based AIC, which can effectively reduce hardware resources and power consumption. In this paper, we also do the hardware platform verification, further verify the hardware physical feasibility of the system. Compared with the existing classification methods based on AIC and SVMs, the proposed method not only has the highest compression rate, but also the highest classification accuracy. To sum up, this method can effectively reduce the processing rate of the information classification system and is expected to be popularized and applied in the low-power, portable wearable system.

6. REFERENCES

[1] Sami Kirolos, Jason Laska, Michael Wakin, Marco Duarte, Dror Baron, Tamer Ragheb, Yehia Massoud, and Richard Baraniuk, "Analog-to-information conversion via random demodulation," in *2006 IEEE Dallas/CAS Workshop on Design, Applications, Integration and Software*, 2006, pp. 71–74.

[2] Joel A. Tropp, Jason N. Laska, Marco F. Duarte, Justin K. Romberg, and Richard G. Baraniuk, "Beyond nyquist: Efficient sampling of sparse bandlimited signals," *IEEE Transactions on Information Theory*, vol. 56, no. 1, pp. 520–544, 2010.

[3] Xiangming Kong, Roy Matic, Zhiwei Xu, Vikas Kukshya, Peter Petre, and Joe Jensen, "A time-encoding machine based high-speed analog-to-digital converter," *IEEE Journal on Emerging and Selected Topics in Circuits and Systems*, vol. 2, no. 3, pp. 552–563, 2012.

[4] Alireza Razavi, Mikko Valkama, and Danijela Cabric, "Compressive detection of random subspace signals," *IEEE Transactions on Signal Processing*, vol. 64, no. 16, pp. 4166–4179, 2016.

[5] John Wright, Allen Y. Yang, Arvind Ganesh, S. Shankar Sastry, and Yi Ma, "Robust face recognition via sparse representation," *IEEE Transactions on Pattern Analysis and Machine Intelligence*, vol. 31, no. 2, pp. 210–227, 2009.

[6] Ching-Yao Chou and An-Yeu Andy Wu, "Low-complexity compressive analysis in sub-eigenspace for ecg telemonitoring system," in *ICASSP 2019 - 2019 IEEE International Conference on Acoustics, Speech and Signal Processing (ICASSP)*, 2019, pp. 7575–7579.

[7] Huai-Ting Li, Ching-Yao Chou, Yi-Ta Chen, Sheng-Hui Wang, and An-Yeu Wu, "Robust and lightweight ensemble extreme learning machine engine based on eigenspace domain for compressed learning," *IEEE Transactions on Circuits and Systems I: Regular Papers*, vol. 66, no. 12, pp. 4699–4712, 2019.

[8] Zhixuan Wang, Ying Liu, Peng Zhou, Zhichao Tan, Haitao Fan, Yihan Zhang, Linxiao Shen, Jiayoon Ru, Yangyuan Wang, Le Ye, and Ru Huang, "A 148-nw reconfigurable event-driven intelligent wake-up system for aiot nodes using an asynchronous pulse-based feature extractor and a convolutional neural network," *IEEE Journal of Solid-State Circuits*, vol. 56, no. 11, pp. 3274–3288, 2021.

[9] Erjia Shi, Xian Tang, and Kong Pang Pun, "A 270 nw switched-capacitor acoustic feature extractor for always-on voice activity detection," *IEEE Transactions on Circuits and Systems I: Regular Papers*, vol. 68, no. 3, pp. 1045–1054, 2021.

[10] Esther Rodriguez-Villegas, Saam Iranmanesh, and Syed Anas Imtiaz, "Wearable medical devices: High-level system design considerations and tradeoffs," *IEEE Solid-State Circuits Magazine*, vol. 10, no. 4, pp. 43–52, 2018.

[11] D.L. Donoho, "Compressed sensing," *IEEE Transactions on Information Theory*, vol. 52, no. 4, pp. 1289–1306, 2006.

[12] Marian Verhelst and Ahmad Bahai, "Where analog meets digital: Analog?to?information conversion and beyond," *IEEE Solid-State Circuits Magazine*, vol. 7, no. 3, pp. 67–80, 2015.

[13] Xinming Liu, Emre Gönültaş, and Christoph Studer, "Analog-to-feature (a2f) conversion for audio-event classification," in *2018 26th European Signal Processing Conference (EUSIPCO)*, 2018, pp. 2275–2279.

[14] Arya A. Rahimi, Huan Hu, Krishnamoorthy Sivakumar, and Subhanshu Gupta, "Energy-efficient serialized walsh-hadamard transform based feature-extraction for information-aware compressive sensing," in *2018 IEEE International Symposium on Circuits and Systems (ISCAS)*, 2018, pp. 1–5.

[15] Chenhui Feng, Hui Qian, and Zhongfeng Wang, "An implementation of pre-quantized random demodulator based on amplitude-to-pulse converter," in *2020 IEEE Computer Society Annual Symposium on VLSI (ISVLSI)*, 2020, pp. 206–211.

[16] G.B. Moody and R.G. Mark, "The impact of the mit-bih arrhythmia database," *IEEE Engineering in Medicine and Biology Magazine*, vol. 20, no. 3, pp. 45–50, 2001.

[17] Noyan Cem Sevüktekin and Andrew C. Singer, "Representation and reconstruction of finite-energy bandlimited signals via pulse-width modulation," *IEEE Transactions on Signal Processing*, vol. 67, no. 19, pp. 5153–5168, 2019.

[18] Y Xue, L Zhang, and B Wang, "Nonlinear feature selection using gaussian kernel svm-rfe for fault diagnosis," *Appl Intell*, vol. 48, pp. 3306–3331, 2018.

[19] C. Venkatesan, P. Karthigaikumar, Anand Paul, S. Satheeskumaran, and R. Kumar, "Ecg signal preprocessing and svm classifier-based abnormality detection in remote healthcare applications," *IEEE Access*, vol. 6, pp. 9767–9773, 2018.